Int J Appl Earth Obs Geoinformation 82 (2019) 101900

Contents lists available at ScienceDirect

Int J Appl Earth Obs Geoinformation

journal homepage: www.elsevier.com/locate/jag

Timing of red-edge and shortwave infrared reflectance critical for early stress detection induced by bark beetle (*Ips typographus*, L.) attack

Haidi Abdullah[a,*], Andrew K. Skidmore[a,b], Roshanak Darvishzadeh[a], Marco Heurich[c,d]

[a] Faculty of Geo-Information Science and Earth Observation (ITC), University of Twente, P.O. Box 217, 7500 AE, Enschede, The Netherlands
[b] Department of Environmental Science, Macquarie University, NSW 2106, Australia
[c] Department of Visitor Management and National Park Monitoring, Bavarian Forest National Park, 94481 Grafenau, Germany
[d] Chair of Wildlife Ecology and Wildlife Management, University of Freiburg, Tennenbacher Straße 4, Freiburg, Germany

ARTICLE INFO

Keywords:
Bark beetle (*Ips typographus*, L.)
Green attack
Norway spruce
Hyperspectral
Foliar biochemical properties
RapidEye
SPOT-5
Temporal analysis

ABSTRACT

Forest disturbance in Europe, induced by European spruce bark beetle *Ips typographus*, L., results in regional-scale dieback. Early stress detection in Norway spruce stands caused by bark beetle infestation at the green attack stage (when trees are yet to show distinct symptoms observable by the human eye) is crucial and can lead to improved forest management and reduced economic losses. This study aims to investigate and understand the dynamics of leaf traits and reflectance of Norway spruce (*Picea abies*) trees during bark beetle attack. Using high-resolution temporal images from RapidEye and SPOT-5 in parallel with the collection of field data, we examined which spectral regions and leaf traits are affected by infestation over time and how they help the discrimination between healthy and infested plots at the early stage of the attack. To achieve this aim, we used a novel approach by targeting both leaf and canopy level. We measured leaf reflectance spectra and six leaf traits (water content, nitrogen, chlorophyll fluorescence, chlorophyll and stomatal conductance) from 66 (30 plots) healthy and 54 (8 plots) infested trees at three consecutive time measurements in the summer of 2015 in the Bavarian Forest National Park. Concurrently, canopy reflectance and spectral vegetation indices (SVIs) were extracted from the selected plots (30 healthy plots) using seven RapidEye images and six SPOT-5 images. For the infested plots, in addition to the field measured plots (8), canopy spectral reflectance were extracted from the reference infestation data (291 plots) obtained through visual interpretation of high-resolution aerial photographs. Results demonstrated significant differences ($p < 0.05$) in the studied leaf traits between healthy and infested samples, and these differences increased with the progression of infestation. We found that leaf and canopy reflectance were significantly higher ($p \leq 0.05$) for the infested trees by bark beetle than the healthy ones in the 'red edge' (680–790 nm) and 'shortwave infrared' (1110–1490 nm) spectrum throughout the infestation event. Our results further demonstrated that the spectral vegetation indices calculated from the red-edge and SWIR spectral bands, such as NDRE, DSWI, LWCI and NDWI, were able to differentiate between healthy and infested trees earlier than the other SVIs. The new insight offered by these results is that the red-edge and SWIR spectral information from multispectral satellites has the potential to considerably improve monitoring and detection of forest stress and has important implications for European field bark beetle management and future studies.

1. Introduction

Insect outbreaks are one of the key natural disturbances in conifer forests that trigger large-scale tree mortality, with noticeable effects on ecosystem services (Aakala et al., 2011; Raffa et al., 2008; Thom and Seidl, 2016). One of the insects that can create large-scale disturbances in short periods of time is the European spruce bark beetle (*Ips typographus,* L.) (hereafter, referred to as the bark beetle) (Fahse and Heurich, 2011). During recent decades, bark beetle frequency and intensity have dramatically increased (Bentz et al., 2010). For example, in the Norway spruce forests in Central Europe, spruce bark beetles have killed a large number of Norway spruce trees in the order of tens of millions of hectares (Lausch et al., 2013a; Meddens et al., 2012; Raffa et al., 2008). Similarly, in British Columbia, Mountain pine beetles (*Dendroctonus ponderosae*) have killed several million hectares of pine trees since 1999 (Aukema et al., 2008; Westfall and Ebata, 2009). Bark beetles and their host trees are susceptible to climatic change, in particular, decreasing precipitation and increasing temperature (Netherer

* Corresponding author.
E-mail address: Rondk_86@yahoo.com (H. Abdullah).

https://doi.org/10.1016/j.jag.2019.101900
Received 14 December 2018; Received in revised form 25 May 2019; Accepted 14 June 2019

and Schopf, 2010). Because the global average temperature is predicted to increase by 1.4–5.8 °C by 2100, enhancements of the intensity and incidence of bark beetle outbreaks are expected (Morris et al., 2018; Netherer and Schopf, 2010; Overbeck and Schmidt, 2012; Seidl et al., 2011). The bark beetle population has rapidly changed from one to three generations per year, as regional and global temperatures have increased (Bentz et al., 2010). Beetle survival rates have also increased during the winter at northern latitudes, particularly in the old spruce forests of northern and Central Europe that have thus far been spared from major outbreaks (Morris et al., 2018; Öhrn, 2012). Furthermore, simulation studies on the bark beetle population have shown an increase in temperature at higher latitudes and have identified high-risk areas for bark beetle outbreaks and related tree mortality in the future (Bentz et al., 2010; Cailleret et al., 2014).

The extensive increment in the harvesting of European conifer forests, due to bark beetle infestation, has resulted in further research that focuses on various underlying forces to reduce further bark beetle outbreaks (Seidl et al., 2011). One of the common techniques used to combat this threat is to cut and remove the infested trees at an early stage to protect nearby unaffected trees (Fahse and Heurich, 2011). This step should be performed during the early phase of the infestation —the so-called 'green attack'—and before beetle larvae are fully developed and able to infest other nearby trees (Wermelinger, 2004). At this stage, the beetles carry pathogenic blue stain fungus (*Ophiostoma* and *Ceratocystis* species) and will transfer it to the host trees. This fungus affects the translocation of nutrients and water within the trunk of an infested tree (Paine et al., 1997; Rohde et al., 1996). As a result, the initial response of the hosted trees by bark beetles is to close their stomata, a process which decreases the water content due to the shutting down of the stem (Edburg et al., 2012). This behaviour (closing stomata) of the infested trees leads to a decrease in photosynthesis as a result of CO_2 limitation (Flexas et al., 2004) and eventual death through water stress.

Traditionally, foresters had to look for early signs of infestation by searching for a dry brown powder that was produced by the bark beetles during the colonisation process when the beetles tunnel under the bark of the trees (Abdullah et al., 2018a). Such a technique, however, is not practical and is inefficient for application in large areas because it is significantly laborious and costly. Remote sensing data and techniques are a useful alternative for effective forest management. The premise of employing remotely sensed data to monitor and identify stressed or insect-infested forests is that the infested trees show symptoms detectable by remote sensing sensors (Chen and Meentemeyer, 2016).

Previous studies have shown the significant potential of remote sensing data for detecting the advanced stages of bark beetle infestation (so-called 'red-attack' and 'grey-attack') (Coops et al., 2006; Filchev, 2012; Franklin et al., 2003; Hais et al., 2009; Havašová et al., 2015; Meddens et al., 2013; Skakun et al., 2003; White et al., 2007, 2006; Wulder et al., 2006). A red-attack is the advanced stage of bark beetle infestation, in which the attacked trees develop stress symptoms by turning their needles' colour from green to yellow to red-brown. Subsequently, the needles fall from the infested trees, and only the grey bark remains; hence, this stage is termed 'grey attack' (Coulson et al., 1985). It is important to note that the early detection (green attack) of a bark beetle attack is crucial for preventing an outbreak, and salvage logging which is performed for loss recovery and appropriate bark beetle management (Fahse and Heurich, 2011).

Timing plays a critical role in remote sensing and field surveys of bark beetle green attack (Wulder et al., 2009). An operational survey has to be performed when the infestation is in its early phase and should consider the temporal field observation associated with beetle biology and the appearance of the symptoms in the tree foliage. In other words, in remote sensing-based surveys of green attack, the swarming event of the beetles must be considered. For example, the European spruce bark beetle (*Ips typographus,* L.) starts to swarm when the air temperature reaches 16.5 °C (Lobinger, 1994; Wermelinger, 2004). To date, the identification of green attack has been less satisfactory due to many biological, technical and logistical constraints/limitations. These issues include the flight activity of the bark beetle, the time duration required for the colonisation process and the period when the infested trees have yet to show distinct symptoms capable of being observed by human eye. Hence, it is important to consider biological as well as logistical factors when using remotely sensed data to detect bark beetle green attack (Wulder et al., 2009).

Numerous studies have focused on using single-date remote sensing data or have compared the utility of different remotely sensed data from different sensors, to detect early infestation stages; hence, very little attention has been paid to investigating the temporal response of trees under bark beetle attack. For example, early detection of a different beetle (*Dendroctonus southern pine beetle* (spp) in lodgepole pine trees) has been investigated by Gimbarzevsky et al. (1992); Murtha (1972) and Murtha and Wiart (1989) using multispectral aerial photographs. However, it has been challenging in these studies to differentiate between green attacked trees and healthy ones. Similarly, Heath (2001) encountered similar challenges when using airborne hyperspectral data from CASI (Compact Airborne Spectrographic Imager). On the other hand, a number of studies have attempted to detect the early stage of *Ips typographus,* L. green attack using different remote sensing data and techniques with limited success. Ortiz et al. (2013) used TerraSAR-X and single-date high-resolution data from the RapidEye satellite. Lausch et al. (2013b) used a single date airborne hyperspectral HyMAP image data for detecting bark beetle green attack. Immitzer and Atzberger (2014) employed WorldView-2 for detection of bark beetle green attack. More recently, Näsi et al. (2018) have used hyperspectral data obtained from an unmanned aerial vehicle (UAV) stress signals induced by bark beetle infestation at the green attack stage.

As mentioned previously, during the colonisation process, the beetles inoculate the host trees with pathogenic fungi, such as *Ophiostoma* and *Cerato-cystis*. Therefore, the infested trees will develop stress symptoms due to changes in biochemical and spectral properties. As a result, the biochemical properties such as leaf water content, chlorophyll, nitrogen, and stomatal conductance are expected to decline within trees colonised by bark beetles (Abdullah et al., 2018a).

Given the above biological and logistical factors, continuous monitoring is essential for investigating and understanding the dynamic characteristics of leaf properties and canopy reflectance under bark beetle infestation. Such observations can (a) provide detailed information regarding the impact of bark beetle on infested trees, (b) could help to develop a case for detection of early-stage bark beetle infestation and guide management actions to prevent greater damage in the forest. In the past, several studies investigated the temporal effect of European spruce bark beetle (*Ips typographus*, L) and mountain pine beetle (*Dendroctonus* spp.) on infested trees using remote sensing data only (Meigs et al., 2011; Meddens et al., 2013 and Immitzer and Atzberger, 2014). However, to date, there have been no studies investigating the temporal effect of European spruce bark beetle (*Ips typographus*, L) attack on infested trees in the early development phase using both field and remote sensing measurements. Therefore, in this study for the first time, we sought to investigate the temporal effect of bark beetle attack on infested trees in the early development phase (green until the red attack stage) using both field and remote sensing data. To do this, we targeted both the foliar and canopy levels by continuously monitoring the changes using temporal field data measurements and temporal remote sensing satellite data from RapidEye and SPOT-5. The combination of field and remote sensing measurements has proved to be very beneficial in our work on European spruce bark beetle attack in the coniferous forests of Europe (Abdullah et al., 2019).

Specifically, the main goals of this study are (i) to analyse the temporal dynamics for a number of leaf traits influenced by bark beetle attack from the beginning of infestation until the advanced stage of

attack (red attack) and (ii) to identify and explore remote sensing time-series indices effective for explaining changes in leaf traits, as well as for detecting early stages of bark beetle infestation.

2. Material and methods

2.1. Study site

The study site is the southern part of Bavarian Forest National Park (BFNP), which is located in south-eastern Germany along the border of the Czech Republic, and it lies between 13°12′9″ E (longitude) and 49°3′19″ N (latitude). The BFNP established in 1970 and extended in 1977, covering an area of 240 km^2. Depending on the elevation in the BFNP, which ranges from 600 m to 1450 m, the mean annual temperature fluctuates between 3.5° and 9 °C, and the total annual precipitation varies from 900 to 1800 mm (Bässler et al., 2008; Heurich et al., 2010).

In the BFNP, three major forest types can be recognised; these are highlands, hillsides, and valleys. The highlands above 1100 m are dominated by Norway spruce (*Picea abies*), and some Mountain ash (*Sorbus aucuparia*); in the hillsides, with elevation between 600–1100 m, is mixed forest including Norway spruce (*Picea abies*), European beech (*Fagus sylvatica*), White fir (*Abies alba*), and Sycamore maple (*Acer pseudoplatanus*); in the valleys, spruce forests exist, including Mountain ash, Norway spruce, and birches (*Betula pendula, Betula pubescens*) (Cailleret et al., 2014;). Since 1984, the forests of BFNP have been affected by the spruce bark beetle (*Ips typographus,* L.), which have caused an extensive disturbance in this region (Lausch et al., 2011).

2.2. Field data collection

In summer 2015, an extensive field survey was conducted to collect field measurements, in which the selected sample trees were visited on three separate occasions (Table 1). We divided the study site into healthy Norway spruce tree stands as well as stands with trees freshly infested by bark beetles. Considering the nature of the forest heterogeneity in tree species, tree age and density, 30 healthy plots were randomly selected. To select the green attacked trees, we conducted an extensive field survey to search for dry brown powder around the trees and eight infested plots were selected (Fig. 1). Within healthy and infested plots, we selected 120 trees (66 healthy and 54 green attacked) to measure foliar properties. The measurements of foliar properties from the selected sample trees (120) were repeated three times (T1, T2, & T3). Part of these data have been used in our earlier study (Abdullah et al., 2018a) while here three consecutive repeated measurements are used.

Bark beetle outbreaks generally occur over the course of several years, and to avoid mixed reflectance from previous years' attacked trees and green attacked trees, only those plots that showed freshly infested or green-attacked trees were considered. A Leica GPS 1200 differential global positioning system (DGPS) (Leica Geosystems AG, Heerbrugg, Switzerland) was used to locate the centre of each plot (Abdullah et al., 2018b, 2019).

From each tree, two to three branches were taken from the upper canopy exposed to sunlight. Because the height of Norway spruce trees reaches 25–30 m, we used a crossbow to shoot an arrow with a fishing line into a branch with sunlit leaves. Full details regarding the use of the crossbow can be found in (Ali et al., 2016a, b). Next, to measure leaf traits, needle samples were removed from collected branches. In the field, total chlorophyll, chlorophyll fluorescence and stomatal conductance were measured. A handheld chlorophyll content meter (CCM) was used to measure both chlorophyll and chlorophyll fluorescence. From each fallen branches, an average of ten readings were immediately taken using the CCM. To measure the needle stomatal conductance, a steady-state instrument (SC-1 Leaf Porometer) was used. This instrument computes stomatal conductance utilising a leaf clip chamber that can monitor the relative humidity (RH%) released from the leaf stomata.

The needle samples were covered by wet paper and placed in a labelled plastic zip-locked bag in order to transport to the laboratory in a portable cooling box and processed within 5 h. In the laboratory, an ASD FieldSepc-3 Pro FR spectrometer equipped with an ASD RT3-3ZC integrating sphere (Analytical Spectral Devices, Inc., Boulder, Co, USA) was used to measure the directional hemispherical reflectance from 350 to 2500 nm for the collected samples. Finally, measurements from branches are averaged for each tree, and then tree measurements were averaged to get the plot leaf reflectance and considered for further analysis. The details concerning the measurements of hemispherical needle reflectance can be found in Abdullah et al. (2018a) and Malenovský et al. (2006). To calculate leaf water content, three grams of fresh needles were taken from each branch and then used to calculate the fresh weight (Fw/g) and leaf surface area (LA cm2) for collected samples using a digital scale and an AMH 350 leaf area meter. The needle samples were then oven-dried for 72 h at 60 °C until a constant weight was obtained. Finally, to measure the nitrogen concentration of the dried needles, an organic elemental analyser (FLASH 2000) was used.

Leaf water content (C_w) was determined using the following equations:

$$C_w\ (g/cm^2) = (Fw - Dw) / LA \quad (1)$$

where Fw, Dw, and A represent fresh leaf weight (g), dry leaf weight (g). The studied leaf traits (total chlorophyll, chlorophyll fluorescence,

Table 1
The leaf traits measured and overview of satellite data acquisition in the Bavarian Forest National Park, 2015. The (✓) are the SPOT-5 data and (•) are the RapidEye data. T1, 2, and 3 represent first, second, and third field measurements, respectively.

Field measurements time	Leaf traits
Time-1 (T1) (15/May To 1/Jun) **Time-2 (T2)** (2/Jun To 18/Jun) **Time-3 (T3)** (20/Jun To 10/July)	Total chlorophyll (Ch mg/m^2) Chlorophyll fluorescence Nitrogen concentration (g/cm^2) Leaf water content (C_w g/cm^2) Stomatal conductance (mmol/(m^2·s) Leaf reflectance spectra (nm)

Satellite data												
RapidEye		•		•	•		•		•	•		•
SPOT-5	✓		✓			✓		✓			✓	✓
	11-May	**13-May**	**05-Jun**	**14-Jun**	**02-July**	**10-July**	**17-July**	**04-Aug**	**06-Aug**	**26-Aug**	**29-Aug**	**13-Sep**

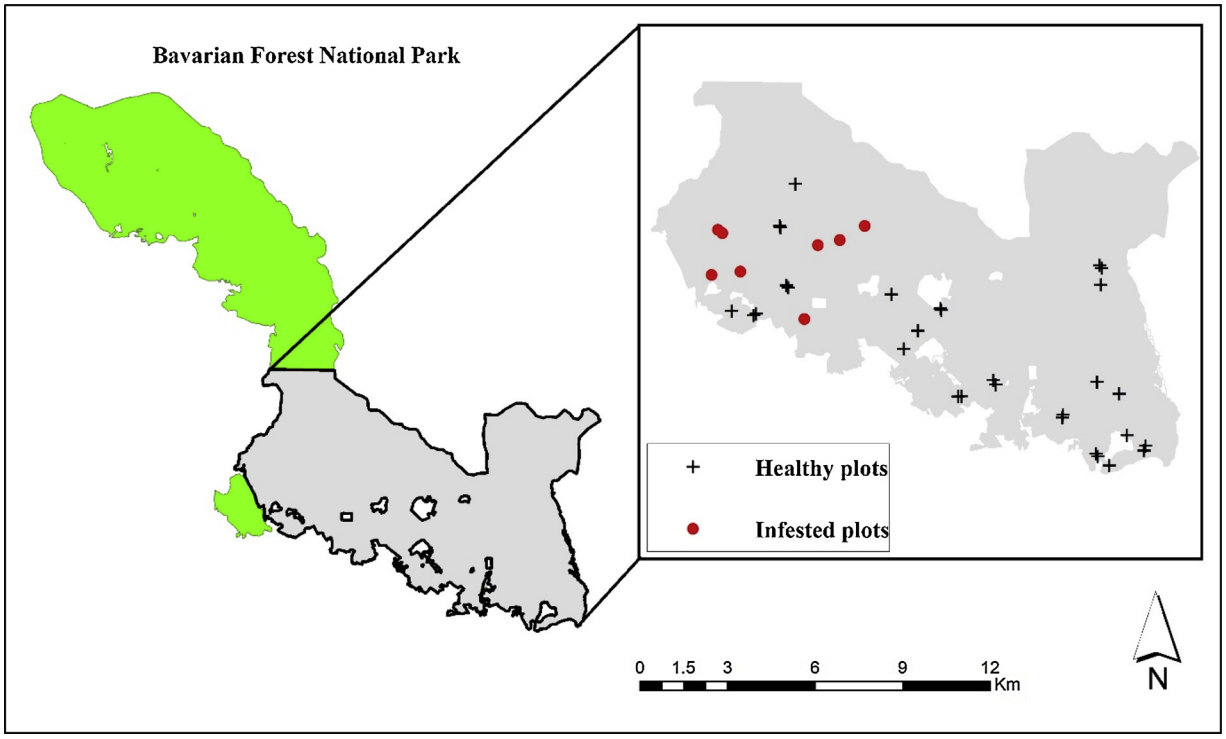

Fig. 1. Distribution of collected sample plots (healthy and infested) during a field campaign in the southern part of Bavarian Forest National Park, Germany.

nitrogen concentration, water content, and stomatal conductance) were continuously measured at three different times for the representative trees (Table 1).

2.3. Satellite imagery

We identified two series of high-resolution multispectral satellite data, namely RapidEye and SPOT-5 (Table 1). The RapidEye orbit system consists of five satellites, each of them collecting radiation in the five spectral bands blue, green, red, red edge and near-infrared (NIR). In this study, seven RapidEye images were captured within the time period from May 2015 to September 2015. They were systematically geo-corrected radiance and orthorectified at 5 m spatial resolution and matched each other with sub-pixel accuracy (RapidEye, 2011; Tyc et al., 2005). Finally, the images were atmospherically and topographically using ATCOR-3 (Richter and Schläpfer, 2012)

For the SPOT-5, we used six images from L2A reflectance product, that provides data with atmospheric and topographic corrections as well as with corresponding masks, clouds, and shadows. It captures data in 4 spectral bands (green, red, near infrared and shortwave infrared). The SPOT-5 L2A has 10 m spatial resolution when acquired within the Take-5 initiative (Meygret, 2007). The full detail about specifications of RapidEye and SPOT-5 sensors are provided in Appendix 1.

2.3.1. Ancillary data (reference disturbance data)

Vector-based reference data of the green attacked areas in 2015 were obtained from the Bavarian Forest National Park (BFNP) administration (Abdullah et al., 2018b). The reference data are produced from aerial colour-infrared (VIS and NIR) images with 0.1 m spatial resolution. The aerial images were obtained during the flight campaign that was carried out in Jun 2016. As mentioned in the earlier section, infested trees exhibit three different stages of damage when it is a host of the bark beetle. These stages are commonly referred to as green, red and grey attacks. The first two stages (green and red) take place within the first 1–6 months after the initial attack (April–May). In contrast, the last stage (grey attack) usually develops within six months to one year after the red attack stage when the needles of the infested trees fall off, and only the grey bark remains. This discolouration of the attacked trees is evident at the canopy level. As a result, the flight campaign (aerial survey) documented the new deadwood (grey attack stage) from the 2015 infestation. For more detailed information regarding the processing and interpretation of aerial images in the BFNP, see Heurich et al. (2009) and Lausch et al. (2013a).

The data were rasterised into 5 m × 5 m grid cells to match with a spatial resolution of RapidEye, and 10 m × 10 m grid cells to match with the spatial resolution of SPOT-5 data. From the rasterised data, 299 infested plots were selected to extract the reflectance value (Fig. 2).

2.3.2. Spectral vegetation indices

Several spectral vegetation indices exist in the literature that are used for the estimation of vegetation biochemical properties (Collins and Woodcock, 1996; Eitel et al., 2006). In this study, spectral vegetation indices linked to measured leaf traits were calculated from the spectral reflectance data collected from the SPOT-5 and RapidEye images (Table 2). The spectral reflectance and SVIs value were extracted from satellite images for the selected 30 healthy and 299 infested sample plots. The value extraction was done using ENVI-IDL5.5 spectral analysis toolbox. From the calculated vegetation indices, time series data stacks were then generated from each sample plot. The time series data were then subjected to further analysis.

2.4. Data analysis

To understand the temporal variations in all the measurements (leaf traits and extracted canopy reflectance data), we first explored the temporal variation from the time-series data (T1–T3) (Table. 1). At the leaf level, mean and standard error values were calculated for both the healthy and infested sample trees to determine the temporal variation in the biochemical components. In addition, we conducted a Student *t*-test to investigate whether the variations in the measured leaf traits were significantly different ($p < 0.05$) between healthy and green attacked samples. Similarly, an unpaired Student *t*-test was used to examine whether the temporal variation in leaf reflectance spectra

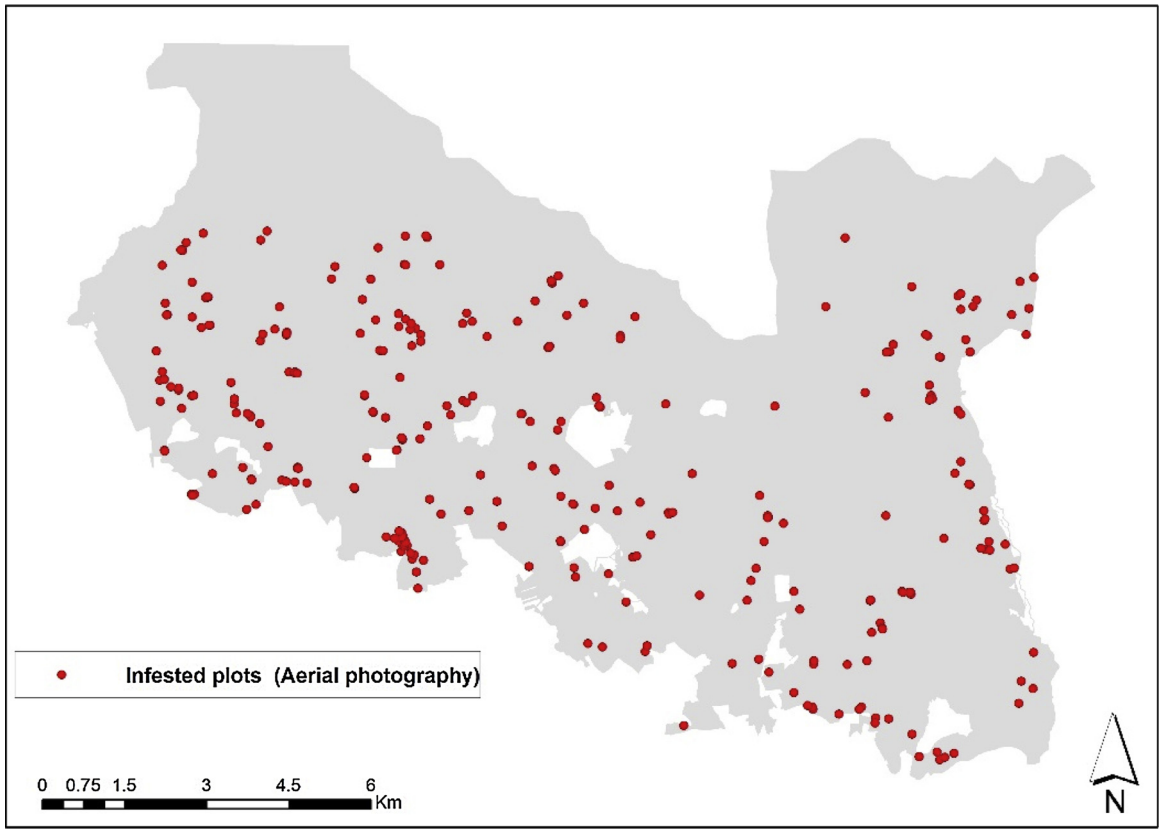

Fig. 2. Illustrates the location of sample plots identified based on ground truth data (aerial photography) in the southern part of Bavarian Forest National Park, Germany.

correlated with the bark beetle infestation and to identify the wavelength regions which were significantly different between the healthy and infested samples.

At the canopy level, box plots and Student *t*-tests were applied. Firstly, a box plot was used to explore temporal variations in the extracted spectral reflectance data in the given years. Secondly, a *t*-test was used to examine whether there were significant differences ($p < 0.05$) in reflectance data between these two sample plots (healthy and infested). Moreover, from the calculated spectral vegetation indices, the mean and standard errors were extracted for each sample plot, and a temporal comparison was made.

Table 2
List of spectral vegetation indices calculated from SPOT-5 and RapidEye data for both healthy and infested sample plots.

Index	Satellite SPOT-5	RapidEye	Equation	Reference
NDVI Normalize difference vegetation indices	✓	✓	$\frac{(NIR - Red)}{(NIR + Red)}$	Tucker (1979)
NDRE Normalize difference red-edge indices	×	✓	$\frac{(NIR - Rededge)}{(NIR + Rededge)}$	Haboudane (2004)
GLI Green leaf index	×	✓	$\frac{2 \times (Green - Red - Blue)}{2 \times (Green + Red - Blue)}$	Gobron et al. (2000)
CIG Chlorophyll index green	✓	✓	$\left(\frac{NIR}{Green}\right) - 1$	Gitelson et al. (2003)
CVI Chlorophyll vegetation index	✓	✓	$NIR\left(\frac{Red}{Green \wedge 2}\right)$	Vincini et al. (2008)
NGRDI Normalize difference Green/red	✓	✓	$\frac{(Green - Red)}{(Green + Red)}$	Hunt et al. (2011)
PBI Plant biochemical index	✓	✓	$\frac{(NIR)}{(Green)}$	This study
RDI Ratio drought index	✓	×	$\frac{(SWIR)}{(NIR)}$	Pinder and McLeod (1999)
NDWI Normalize difference water index	✓	×	$\frac{(NIR - SWIR)}{(NIR + SWIR)}$	Hardisky et al. (1983)
DSWI Disease stress water index	✓	×	$\frac{(NIR + Green)}{(SWIR + Red)}$	Galvao et al. (2005)
LWCI Leaf water content index	✓	×	$\frac{log(1 - (NIR - SWIR))}{-log(1 - (NIR - SWIR))}$	COHEN (1991)

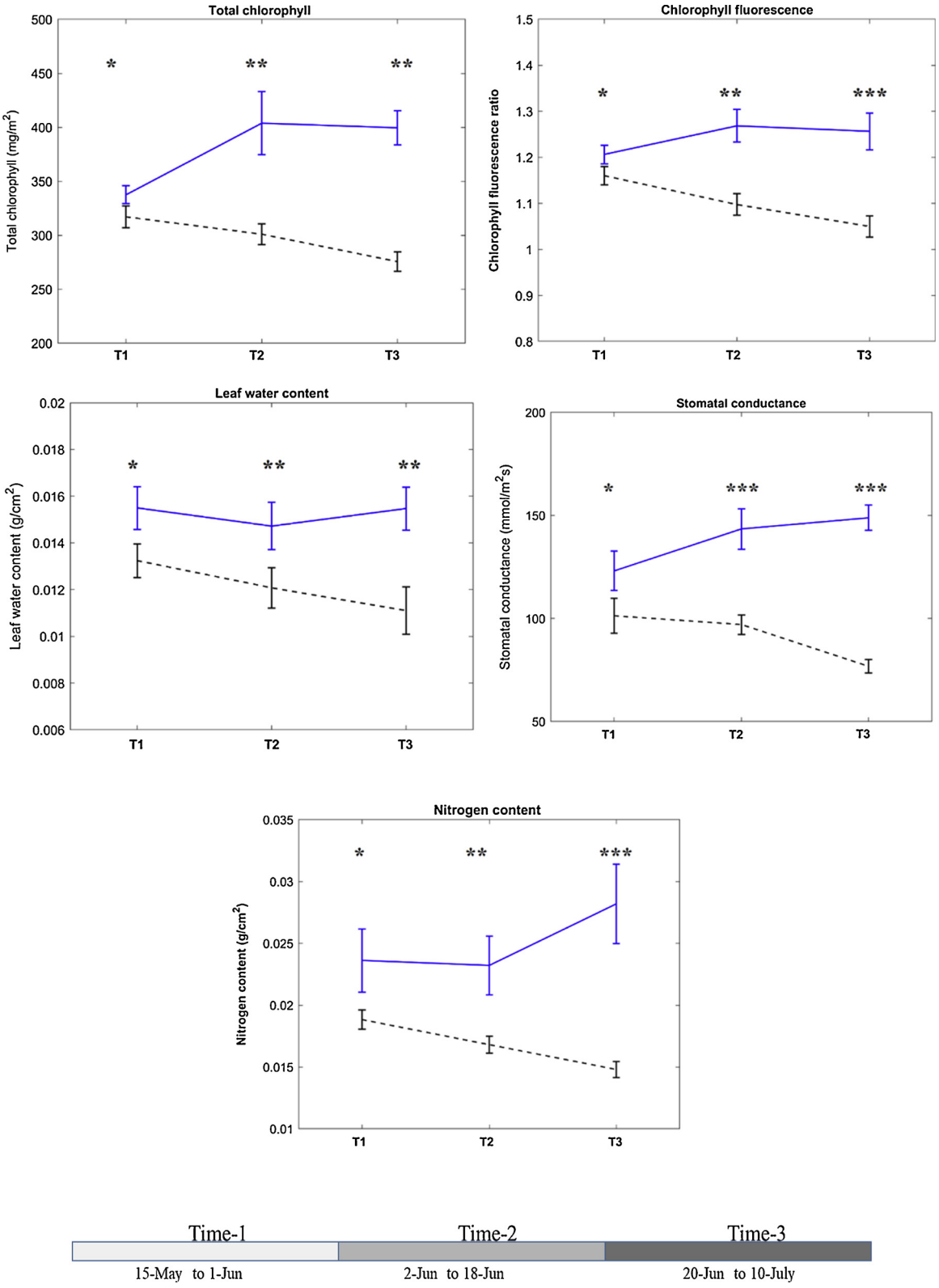

Fig. 3. Temporal variation of the measured leaf traits for healthy and infested samples. Blue and black lines represent healthy and infested plots, respectively. T1, T,2 and T3 represent first, second, and third measurements, respectively. (*) Hardly significant, (**) significant, (***) Strongly significant. The error bars show the (mean and standard error) of each data set (leaf traits). (For interpretation of the references to colour in this figure legend, the reader is referred to the web version of this article).

3. Results

3.1. Temporal response of measured leaf traits under bark beetle infestation

The results of the temporal variation demonstrated that there was a clear distinction between healthy and infested sample trees from the Time-1 (T1) to Time-3 (T3) measurements (Fig. 3). In the healthy leaves, the mean of the total chlorophyll concentrations were 337, 403, and 399 mg/m^2 at T1, T2 and T3, respectively. However, for the infested samples, the mean of the total chlorophyll concentrations was lower, *viz*. 317, 301, and 275 mg/m^2, respectively. Similar trends were observed for the other leaf traits, where all measured leaf traits values decreased within the infested samples from T1 to T3. For example, the stomatal conductance which was measured at the beginning of the infestation at T1 for the infested leaf was higher when compared to the ones at T3, whereas, for the healthy leaves, the opposite result was observed.

This was further confirmed by the results of the Student *t*-test, which showed a significant difference ($p < 0.05$) between healthy and infested samples in all measured leaf traits (chlorophyll fluorescence, chlorophyll, nitrogen concentration, stomatal conductance, and leaf water content). At the beginning of the infestation (T1), the differences were smaller between the two sample groups (healthy and infested) for all studied leaf traits. However, there was a larger difference between the infested and healthy needles at T2 and T3, as the infested trees developed signs of stress (Fig. 3).

Further analysis of the leaf spectral reflectance spectra values showed that the mean reflectance spectra of green attacked samples was higher than for the healthy ones in the visible and shortwave infrared region (Fig. 4). The difference ($p < 0.05$) was stronger during T2 and T3, as the infested trees showed increased stress symptoms.

3.2. Temporal response of canopy spectral data to bark beetle infestation

We assessed the response of canopy reflectance to bark beetle attack employing a time series of remotely sensed images from RapidEye and SPOT-5. The reflectance data were extracted from each image and for both sets of satellite data (RapidEye and SPOT-5). We found a symmetrical change of reflectance data for both sets of satellite data (Figs. 5 and 6). For example, for the RapidEye imagery, the reflectance of red-edge and NIR bands were higher for the infested plots than the healthy ones on May 13. The variation of these two spectral bands increased with the progression of infestation on July 2 and the later images. Moreover, a Student *t*-test of spectral bands revealed similar findings, as the red-edge was significantly different ($p < 0.05$) between healthy and infested plots for all RapidEye imagery considered in this study, while the variation in NIR between healthy and infested plots showed a significant difference ($p < 0.05$) from July 2 and later (Fig. 5). For the SPOT-5 imagery, the reflectance of SWIR appears to be the most sensitive to the bark beetle stressor, as it was significantly different ($p < 0.05$) from May 11 onwards (Fig. 6).

Further analysis regarding the SVIs shows that there was a big overlap between healthy and infested plots in May for both RapidEye and SPOT-5. However, as infestation progresses, this variation becomes larger and more distinct (Figs. 7 and 8). For the RapidEye data, the difference between the healthy and infested plots by means of spectral vegetation indices values started to change from July 2nd using NDRE and NGRDI, while the other indices started to enlarge the variation at the later dates considered in this study (Fig. 7). A similar result was found using a reflectance difference index, as the red-edge and NIR bands became statistically different from May, becoming progressively more pronounced at later dates.

Using SPOT-5, the spectral vegetation indices calculated from the combination of SWIR and other spectral bands, such as DSWI, LWCI and NDWI, exhibited a larger difference between the healthy and infested plots at the earlier stage of infestation (Fig. 8). This is also confirmed in the result of the Student *t*-test analysis, where the SWIR was significantly different ($P < 0.05$) for all dates considered in this study.

4. Discussion

In this study, we demonstrated that the measured leaf traits and leaf reflectance spectra from infested trees differed significantly ($p \leq 0.05$) from healthy ones during T1, T2, and T3 measurements (Figs. 3 and 4). Furthermore, the red-edge and SWIR spectral bands from RapidEye and SPOT-5 were influential in the separating between healthy and infested plots. Moreover, we found that red-edge and SWIR bands maintained their sensitivity for monitoring and detecting bark beetle infestation from the early to the advanced stages of infestation (Figs. 5 and 6).

The absolute difference in measured leaf traits between the healthy and infested trees increased from T1 to T3. In particular, stomatal conductance and chlorophyll fluorescence exhibited significant differences between the healthy and infested trees (Fig. 3). A possible explanation for this result might be that the initial impact of bark beetles on the infested trees shuts down the translocation of water in the tree due to the blue stain fungi introduced to the trees during the infestation process. Because the hydraulic systems of plant and stomatal conductance are closely correlated with each other (Ewers et al., 2007), infested trees tend to close their stomata to preserve water. Therefore, stomatal closure is the first sign of stress that induces the physiological response of infested trees to preserve water. It is well-known that physiological factors, such as plant water content, can control the

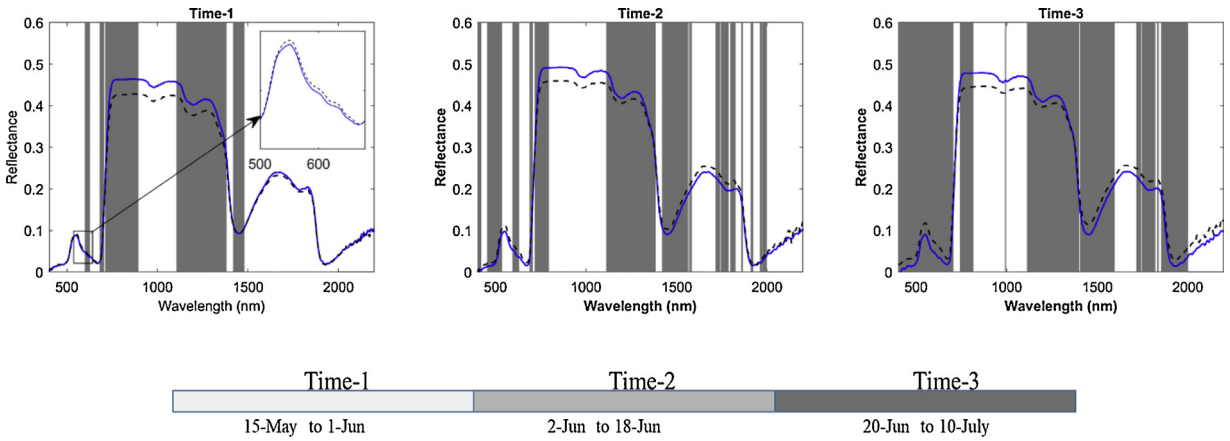

Fig. 4. Mean reflectance spectra of healthy and green attacked leaves at three consecutive repeated time measurements in the summer of 2015. Blue and black lines represent healthy and infested leaves, respectively. The wavebands, where there is a significant difference between healthy and green attacked leaf spectra, are presented in Gray. (For interpretation of the references to colour in this figure legend, the reader is referred to the web version of this article).

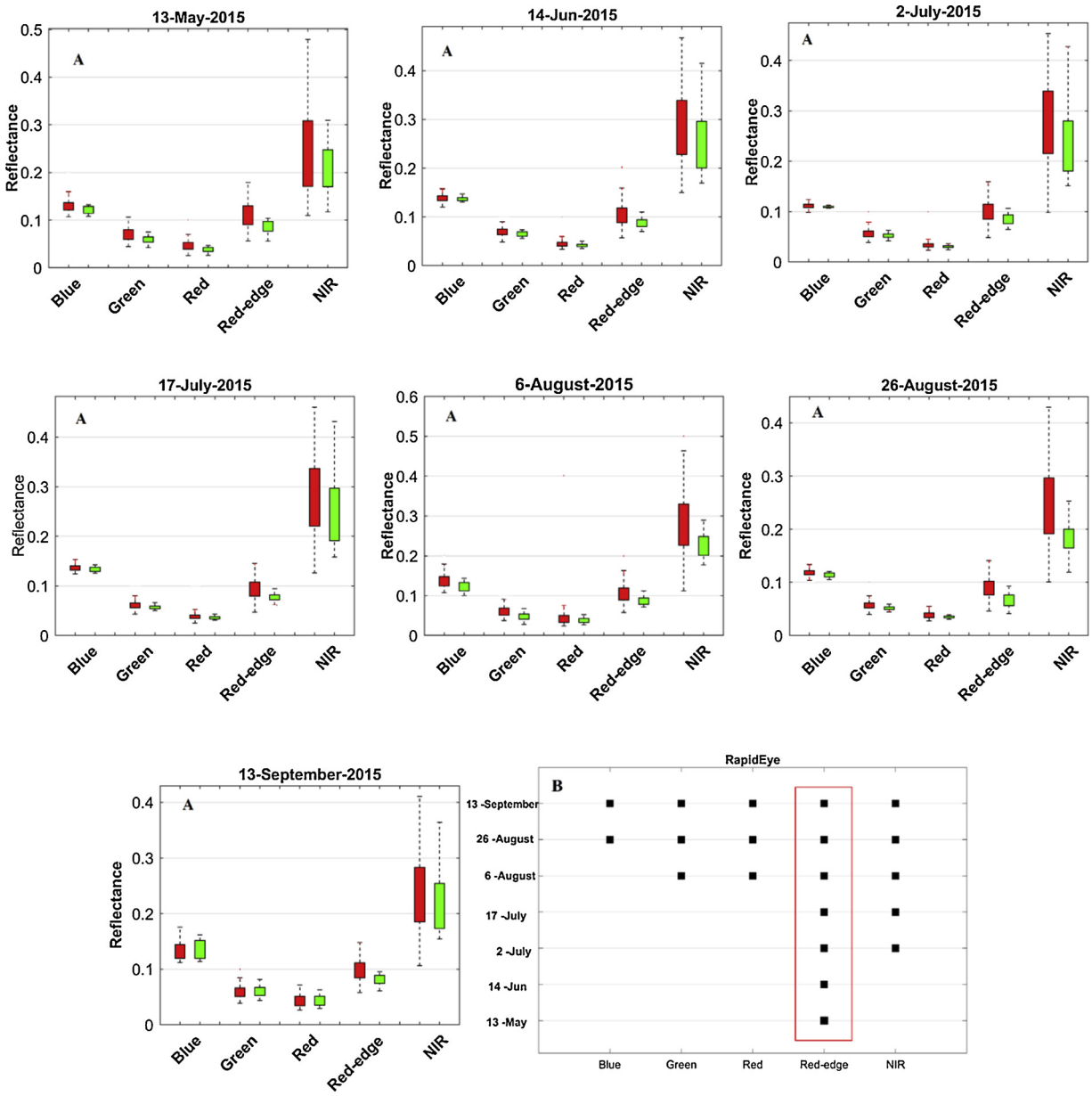

Fig. 5. (A) Temporal variation of canopy reflectance for healthy and infested plots in the Bavarian Forest National Park using RapidEye satellite data. Red and Green boxes represent infested and healthy plots, respectively (B) Unpaired *t*-test canopy reflectance between healthy and infested samples. Dark squares indicate spectral wavebands that were significantly different ($P \leq 0.05$). The red box shows the spectral region that was significantly different overall temporal data considered in this study. The ends of whiskers show the min and max value for each spectral band. (For interpretation of the references to colour in this figure legend, the reader is referred to the web version of this article).

temperature of plants through the stomatal transpiration process (Oerke et al., 2006). Moreover, the stomatal closure leads to a drop in photosynthesis activity due to the CO_2 limitation, and, therefore, the chlorophyll fluorescence decreases (Flexas et al., 2004; Zweifel et al., 2009). Hence, the distinct variation observed in stomatal conductance between healthy and infested trees is attributed to differences in the measured leaf traits—in particular, leaf water content and chlorophyll fluorescence (Fig. 3). These findings match those observed in earlier studies that the initial impact of mountain pine beetles on infested trees causes a drop in the sapwood moisture and, hence, stomatal closure (Yamaoka et al., 1990). Likewise, our findings are in agreement with those of (Cheng et al., 2010), who studied the impact of a similar species, the mountain pine beetle (*Dendroctonus spp*) on the leaf water content of lodgepole pine using hyperspectral data.

Another important finding at the leaf level was that the difference in reflectance spectra between healthy and infested samples increased with the progression of infestation from T1 to T3 (Fig. 4). Noticeable changes were perceived at the visible wavelengths, in particular, from 680 to 790 nm and in the shortwave infrared wavelengths 1110–1490 nm. The reflectance of the infested leaves in the visible spectrum from T1 was distinctly higher than that of the healthy ones. This result was likely due to having significantly ($p < 0.05$) lower chlorophyll in infested leaves than the healthy leaves from T1 to T3, causing lower absorption and higher scattering in the visible wavelengths (Fig. 3) (Carter and Knapp, 2001; Zhang et al., 2008). This confirms the low chlorophyll regions observed in Darvishzadeh et al. (2019).

Furthermore, we reported that the reflectance of the healthy leaves was higher in the NIR region and lower in SWIR than that observed in the green attacked ones. Physically, the leaf reflectance is a function of

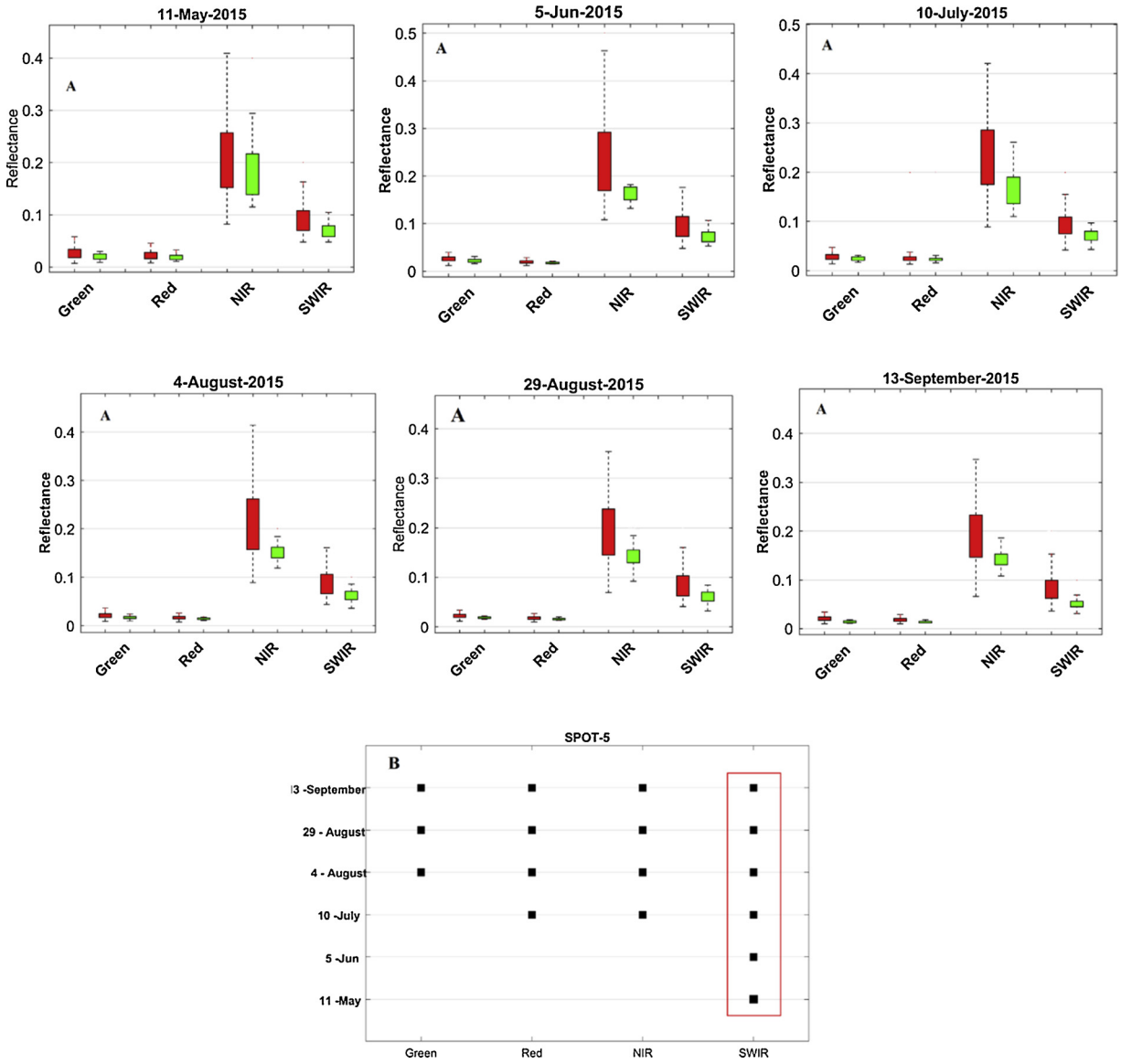

Fig. 6. (A) Temporal variation of reflectance spectra for healthy and infested plots in the Bavarian Forest National Park using SPOT-5 satellite data. Red and Green boxes represent infested and healthy plots, respectively (B) Unpaired *t*-test of canopy reflectance between healthy and infested samples. Dark squares indicate spectral wavebands that were significantly different ($P \leq 0.05$). The red box shows the spectral region that was significantly different overall temporal data considered in this study. The ends of whiskers show the min and max value for each spectral band. (For interpretation of the references to colour in this figure legend, the reader is referred to the web version of this article).

dry matter, water content, chlorophyll and internal leaf structure (leaf thickness) (Ali et al., 2016a, b; Pu and Gong, 2011; Slaton et al., 2001; Darvishzadeh et al., 2019). Hence, the observed reflectance pattern of the infested samples may have been due to the decrease in water content (Fig. 3), which is caused by bark beetle infestation. This finding is in agreement with our earlier study (Abdullah et al., 2019), which demonstrated a significant decrease in water content within infested trees during the early attack stage.

Similarly, at the canopy level, both red-edge and SWIR bands from RapidEye and SPOT-5, respectively, showed a significant difference between the healthy and infested sites for all the dates considered in this study (Figs. 5 and 6). When implemented as a time series, they showed distinct temporal variation in reflectance and indices values between the healthy and infested sites, especially during the later stages of infestation. For example, the NDRE calculated based on the combination of the red-edge and NIR bands is shown to be more sensitive than the other SVIs due to the stress induced by bark beetle infestation. The NDRE is known to detect stress or any forest health decrease earlier than NDVI (Eitel et al., 2011). In our study, the NDRE started to differentiate between the healthy and infested plots from 2nd July, while the other SVIs showed a difference almost one month later (Fig. 7). This result is in agreement with our earlier findings (Abdullah et al., 2018b) in which the NDRE calculated from the Sentinel-2 imagery possessed the most sensitive indices to differentiate between the healthy and green attacked sample plots.

Moreover, as shown in Figs. 5 and 6, there are visible differences between spectral responses of two sensors (RapidEye and SPOT-5) in the green and near NIR spectral region, potentially due to differences in their spatial resolution, spectral width and location of the bands (Appendix 1). As can be seen from Figs. 5 and 6, the spectral differences between healthy and infested plots were more obvious for RapidEye data compared to SPOT-5 over the green and NIR spectral region. This observation confirms the importance of high spatial resolution data from RapidEye in the study of bark beetle green attack.

All the indices, such as DSWI, NDWI and LWCI, which employed the SWIR bands, were mostly sensitive to stress caused by variations in

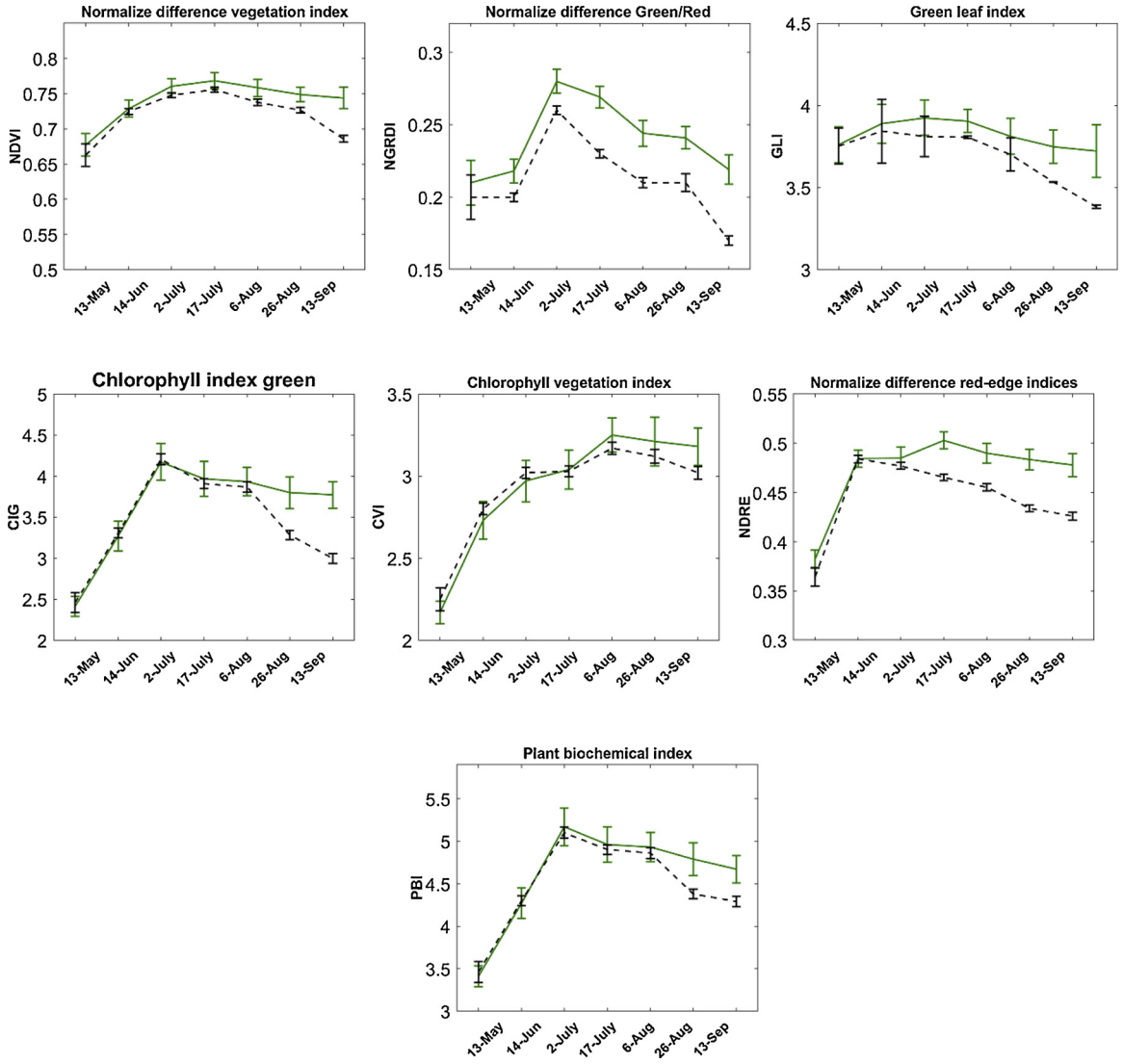

Fig. 7. Temporal variation of studied spectral vegetation indices for healthy and infested plots in the Bavarian Forest National Park using RapidEye satellite data. Green and black lines represent healthy and infested plots, respectively. (For interpretation of the references to colour in this figure legend, the reader is referred to the web version of this article).

water content and were able to discriminate healthy from infested sites. For example, the DSWI and NDWI showed significant differences between the two groups on June 5th and July 10th, respectively. This is due to the significantly lower water content ($P < 0.05$) of the infested samples, and, therefore, their spectral reflectance in the SWIR region were highly affected (Figs. 3 and 6). This also accords with our earlier observation (Abdullah et al., 2018b), which showed the SWIR bands from Sentinel-2 and Landsat-8 were sensitive to detecting bark beetle infestation at the early phase of the attack. Likewise, Foster et al. (2017) identified the shortwave infrared region as key for detecting the early stages of beetle infestation in Engelmann spruce trees.

Based on the temporal variations in the canopy reflectance values and measured SVIs, here we identified for the first time in the European situation (and in contrast to earlier works in the US) that mid-June to the beginning of July is an appropriate time frame for the early stress detection induced by bark beetle infestation (Figs. 4–6). This is the most initial period when the spectral difference between infested and healthy plots peaks. Although this time period may be slightly late for appropriate bark beetle management, our study has however shown the impending role of multispectral satellite (RapidEye and SPOT-5) data for monitoring and detecting forest stress induced by bark beetle attacks, and thus, has important implications for European field bark beetle management and future studies. However, it is important to note that data captured by satellite platforms often have some limitations with respect to being applied for bark beetle green attack detection. The technical and practical limitations such as the sensor specification in terms of spatial, spectral, temporal and radiometric resolution can lead to significant errors and make the data less appropriate for analysis of bark beetle green attack. As a result, further research is essential to explore the potential of other remote sensing platforms such as unmanned aerial vehicles (UAVs), airborne and spaceborne hyperspectral sensors in detecting canopy reflectance changes due to bark beetle infestation during the early stage of an attack. Furthermore, the future of hyperspectral remote sensing is promising, considering forthcoming launches of hyperspectral satellites. There are a number of hyperspectral satellites planned to be launched in the near and distant future such as EnMap, CHIME and HyspIRI. These missions will provide a better opportunity for bark beetle green attack detection.

Not only spaceborne hyperspectral satellites but today other remote-sensing platforms such as UAVs also offer significant potential concerning future remote-sensing applications in forest management. Currently, UAVs can collect data at low altitude and provide high-quality data comparable to airborne sensors. The UAV technology has developed at a significantly rapid pace, and today, different sensors can

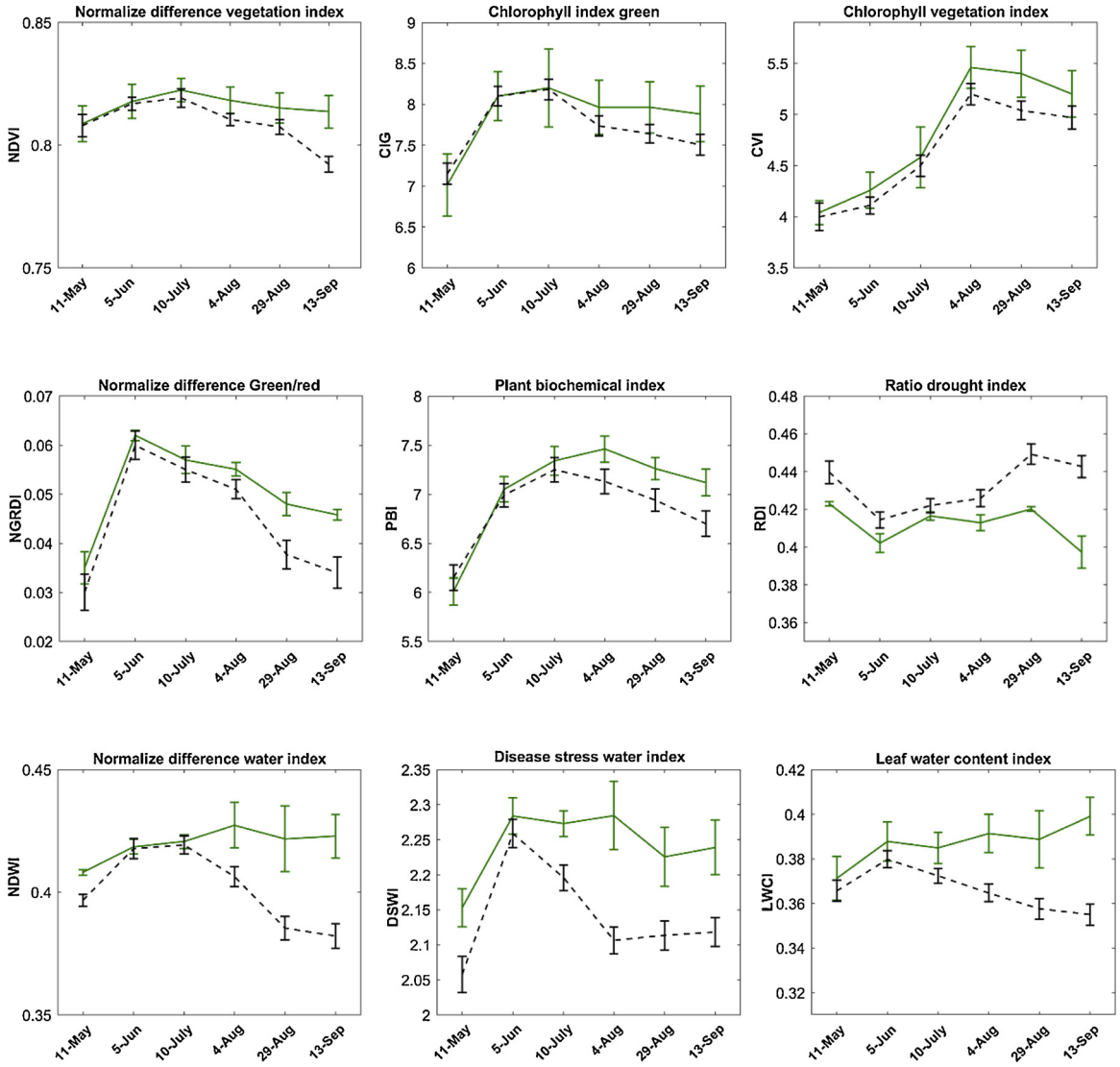

Fig. 8. Temporal variation of studied spectral vegetation indices for healthy and infested plots in the Bavarian Forest National Park using SPOT-5 satellite data. Green and black lines represent healthy and infested plots, respectively. (For interpretation of the references to colour in this figure legend, the reader is referred to the web version of this article).

be attached to UAVs onboard such as positioning sensors (GPS), inertial navigation sensors (INS), micro-electro-mechanical systems (MEMS), gyroscopes, accelerometers and altitude sensors (AS), all of which allow for the realization of remote sensing missions. Moreover, various sensors such as multispectral, hyperspectral, LIDAR and thermal cameras can be installed onto UAV platforms. As a result, recent data collected by UAVs are being widely used for forest management practices. Furthermore, there is a growing interest in the forest management community in using UAVs as a promising and decision-support tool for forest disturbance studies, including bark beetle infestation management. Soon, UAVs can potentially fill the gap between satellite/airborne platforms with 'ground truth' data collected using ASD field spectrometers to study detection of bark beetle at the green attack stage.

5. Conclusion

This study presents an innovative approach to investigate the temporal response of leaf properties and canopy reflectance spectra to European bark beetle infestation using a temporally dense time series of seven RapidEye senses and six SPOT-5 senses in parallel with the collection of field data at three consecutive repeated time measurements. Remote-sensing-based SVIs complemented the ground data collected, providing additional information to help characterise the temporal response of infested trees through time and across the landscape. In conclusion, our key concept is that we show for the first time that:

- All measured leaf traits from infested trees differed significantly from healthy trees during Time-1, -2, and -3 measurements.
- The red-edge and SWIR were important spectral regions at both leaf and canopy levels for detecting subtle changes in Norway spruce trees due to bark beetle infestation.
- The earliest period at which the spectral difference between infested and healthy plots peaks is mid-June to the beginning of July.

We recommend that further studies should investigate different remote sensing datasets and monitor over a longer period to show the relationship between bark beetle infestation and the changes in biochemical variables and spectral reflectance more clearly.

Acknowledgments

This research received financial support from the EU Erasmus

Mundus Salam-2 and was co-funded by Natural Resources Department, Faculty of Geo-Information Science and Earth Observation (ITC), University of Twente, the Netherlands. Thanks also go to the Bavarian Forest National Park staff for approving access to the test site and providing field and camping facilities. The authors extend their appreciation for the great support during the laboratory measurements from the GeoScience Laboratory at ITC Faculty, University of Twente.

Appendix 1

RapidEye L2A		Acquisition date in 2015	Cloud coverage %
Spectral range (nm)	Blue : 440 – 510	13-May	1.4
	Green : 520 – 590	14-Jun	10.1
	Red 630 : – 685	02-Jul	0
	Red-Edge : 690 – 730	17-Jul	0
	NIR : 760 – 850	06-Aug	1
		26-Aug	1
		13-Sep	5.6
Spatial resolution	6.5 m resampled to (5 m)		
Radiometric resolution	12 bit		
SPOT-5			
Spectral range (nm)	Pan: 480–710	11-May	0.65
	Green: 500–590	5-Jun	1.28
	Red: 610–680	10-July	9.15
	NIR: 780–890	4-Aug	0.76
	SWIR: 1.580–1.750 nm		
		29-Aug	2.72
		13-Sep	0.23
Spatial resolution	10 m :- Green, red and NIR		
	5 m :- panchromatic		
	20 m :- SWIR (resampled to 10 m)		
Radiometric resolution	8 bit		

References

Aakala, T., Kuuluvainen, T., Wallenius, T., Kauhanen, H., 2011. Tree mortality episodes in the intact Picea abies-dominated taiga in the Arkhangelsk region of northern European Russia. J. Veg. Sci. 22 (2), 322–333.

Abdullah, H., Darvishzadeh, R., Skidmore, A., Heurich, M., 2019. Sensitivity of landsat-8 OLI and TIRS data to foliar properties of early stage bark beetle (Ips typographus, L.) infestation. Remote Sens. (Basel) 11 (4).

Abdullah, H., Darvishzadeh, R., Skidmore, A.K., Groen, T.A., Heurich, M., 2018a. European spruce bark beetle (Ips typographus, L.) green attack affects foliar reflectance and biochemical properties. Int. J. Appl. Earth Obs. Geoinf. 64, 199–209.

Abdullah, H., Skidmore, A.K., Darvishzadeh, R., Heurich, M., Pettorelli, N., Disney, M., 2018b. Sentinel-2 accurately maps green-attack stage of European spruce bark beetle (Ips typographus, L.) compared with Landsat-8. Remote Sens. Ecol. Conserv. 5 (1), 87–106.

Ali, A.M., Darvishzadeh, R., Skidmore, A.K., Duren, I.V., 2016a. Effects of canopy structural variables on retrieval of leaf dry matter content and specific leaf area from remotely sensed data. Ieee J. Sel. Top. Appl. Earth Obs. Remote. Sens. 9 (2), 898–909.

Ali, A.M., Darvishzadeh, R., Skidmore, A.K., Duren, I.V., Heiden, U., Heurich, M., 2016b. Estimating leaf functional traits by inversion of PROSPECT: assessing leaf dry matter content and specific leaf area in mixed mountainous forest. Int. J. Appl. Earth Obs. Geoinf. 45, 66–76.

Aukema, B.H., Carroll, A.L., Zheng, Y., Zhu, J., Raffa, K.F., Dan Moore, R., Stahl, K., Taylor, S.W., 2008. Movement of outbreak populations of mountain pine beetle: influences of spatiotemporal patterns and climate. Ecography 31 (3), 348–358.

Bässler, C., Förster, B., Moning, C., Müller, J., 2008. The BIOKLIM-Project: biodiversity research between climate change and wilding in a temperate montane forest–the conceptual framework. Waldökologie, Landschaftsforschung und Naturschutz 7, 21–33.

Bentz, B.J., Régnière, J., Fettig, C.J., Hansen, E.M., Hayes, J.L., Hicke, J.A., Kelsey, R.G., Negrón, J.F., Seybold, S.J., 2010. Climate change and bark beetles of the Western United States and Canada: direct and indirect effects. BioScience 60 (8), 602–613.

Cailleret, M., Heurich, M., Bugmann, H., 2014. Reduction in browsing intensity may not compensate climate change effects on tree species composition in the Bavarian Forest National Park. For. Ecol. Manage. 328, 179–192.

Carter, G.A., Knapp, A.K., 2001. Leaf optical properties in higher plants: linking spectral characteristics to stress and chlorophyll concentration. Am. J. Bot. 88 (4), 677–684.

Chen, G., Meentemeyer, R., 2016. Remote Sensing of Forest Damage by Diseases and Insects. pp. 145–162.

Cheng, T., Rivard, B., Sánchez-Azofeifa, G.A., Feng, J., Calvo-Polanco, M., 2010. Continuous wavelet analysis for the detection of green attack damage due to mountain pine beetle infestation. Remote Sens. Environ. 114 (4), 899–910.

COHEN, W., 1991. Response of vegetation indices to changes in three measures of leaf water stress. Photogramm. Eng. Remote Sensing 57 (2), 195–202.

Collins, J.B., Woodcock, C.E., 1996. An assessment of several linear change detection techniques for mapping forest mortality using multitemporal landsat TM data. Remote Sensing of Environment 56 (1), 66–77.

Coops, N.C., Johnson, M., Wulder, M.A., White, J.C., 2006. Assessment of QuickBird high spatial resolution imagery to detect red attack damage due to mountain pine beetle infestation. Remote Sens. Environ. 103 (1), 67–80.

Coulson, R.N., Amman, G.D., Dahlsten, D.L., De Mars Jr., C., Stephen, F., 1985. Forest-bark Beetle Interactions: Bark Beetle Population Dynamics. Integrated Pest Management in Pine-bark Beetle Ecosystems. John Wiley & Sons, New York, pp. 61–80.

Darvishzadeh, R., Skidmore, A., Abdullah, H., Cherenet, E., Ali, A., Wang, T., Nieuwenhuis, W., Heurich, M., Vrieling, A., O'Connor, B., 2019. Mapping leaf chlorophyll content from sentinel-2 and RapidEye data in spruce stands using the invertible forest reflectance model. Int. J. Appl. Earth Obs. Geoinf. 79, 58–70.

Edburg, S.L., Hicke, J.A., Brooks, P.D., Pendall, E.G., Ewers, B.E., Norton, U., Gochis, D., Gutmann, E.D., Meddens, A.J., 2012. Cascading impacts of bark beetle-caused tree mortality on coupled biogeophysical and biogeochemical processes. Front. Ecol. Environ. 10 (8), 416–424.

Eitel, J.U., Gessler, P.E., Smith, A.M., Robberecht, R., 2006. Suitability of existing and novel spectral indices to remotely detect water stress in *Populus* spp. Forest Ecology and Management 229 (1-3), 170–182.

Eitel, J.U.H., Vierling, L.A., Litvak, M.E., Long, D.S., Schulthess, U., Ager, A.A., Krofcheck, D.J., Stoscheck, L., 2011. Broadband, red-edge information from satellites improves early stress detection in a New Mexico conifer woodland. Remote Sens. Environ. 115 (12), 3640–3646.

Ewers, B., Mackay, D., Samanta, S., 2007. Interannual consistency in canopy stomatal conductance control of leaf water potential across seven tree species. Tree Physiol. 27 (1), 11–24.

Fahse, L., Heurich, M., 2011. Simulation and analysis of outbreaks of bark beetle infestations and their management at the stand level. Ecol. Modell. 222 (11), 1833–1846.

Filchev, L., 2012. An assessment of European spruce bark beetle infestation using worldview-2 satellite data. Proc. of European SCGIS Conf.:"Best Practices: Application of GIS Technologies for Conservation of Natural and Cultural Heritage Sites. pp. 9–16.

Flexas, J., Bota, J., Cifre, J., Mariano Escalona, J., Galmés, J., Gulías, J., Lefi, E.K., Florinda Martínez-Cañellas, S., Teresa Moreno, M., RIBAS-CARBÓ, M., 2004. Understanding down-regulation of photosynthesis under water stress: future prospects and searching for physiological tools for irrigation management. Ann. Appl. Biol. 144 (3), 273–283.

Foster, A.C., Walter, J.A., Shugart, H.H., Sibold, J., Negron, J., 2017. Spectral evidence of early-stage spruce beetle infestation in Engelmann spruce. For. Ecol. Manage. 384, 347–357.

Franklin, S.E., Wulder, M.A., Skakun, R.S., Carroll, A.L., 2003. Mountain pine beetle red-attack forest damage classification using stratified landsat TM data in british Columbia, Canada. Photogrammetric Engineering & Remote Sensing 69 (3), 283–288.

Galvao, L.S., Formaggio, A.R., Tisot, D.A., 2005. Discrimination of sugarcane varieties in Southeastern Brazil with EO-1 Hyperion data. Remote Sens. Environ. 94 (4), 523–534.

Gimbarzevsky, P., Dawson, A.F., Van Sickle, G., 1992. Assessment of Aerial Photographs

and Multi-spectral Scanner Imagery for Measuring Mountain Pine Beetle Damage. 333. .
Gitelson, A.A., Viña, A., Arkebauer, T.J., Rundquist, D.C., Keydan, G., Leavitt, B., 2003. Remote estimation of leaf area index and green leaf biomass in maize canopies. Geophys. Res. Lett. 30 (5).
Gobron, N., Pinty, B., Verstraete, M.M., Widlowski, J.-L., 2000. Advanced vegetation indices optimized for up-coming sensors: design, performance, and applications. Ieee Trans. Geosci. Remote. Sens. 38 (6), 2489–2505.
Haboudane, D., 2004. Hyperspectral vegetation indices and novel algorithms for predicting green LAI of crop canopies: modeling and validation in the context of precision agriculture. Remote Sens. Environ. 90 (3), 337–352.
Hais, M., Jonášová, M., Langhammer, J., Kučera, T., 2009. Comparison of two types of forest disturbance using multitemporal Landsat TM/ETM + imagery and field vegetation data. Remote Sens. Environ. 113 (4), 835–845.
Hardisky, M., Klemas, V., Smart, M., 1983. The influence of soil salinity, growth form, and leaf moisture on the spectral radiance of. Spartina alterniflora 49, 77–83.
Havašová, M., Bucha, T., Ferenčík, J., Jakuš, R., 2015. Applicability of a vegetation indices-based method to map bark beetle outbreaks in the high Tatra Mountains. Ann. For. Res. 58 (2).
Heath, J., 2001. The Detection of Mountain Pine Beetle Green Attacked Lodgepole Pine Using Compact Airborne Spectrographic Imager (CASI) Data. University of British Columbia.
Heurich, M., Beudert, B., Rall, H., Křenová, Z., 2010. National Parks As Model Regions for Interdisciplinary Long-term Ecological Research: the Bavarian Forest and Šumavá National Parks Underway to Transboundary Ecosystem Research, Long-term Ecological Research. Springer, pp. 327–344.
Heurich, M., Ochs, T., Andresen, T., Schneider, T., 2009. Object-orientated image analysis for the semi-automatic detection of dead trees following a spruce bark beetle (Ips typographus) outbreak. Eur. J. For. Res. 129 (3), 313–324.
Hunt, E.R., Daughtry, C., Eitel, J.U., Long, D.S., 2011. Remote sensing leaf chlorophyll content using a visible band index. Agron. J. 103 (4), 1090–1099.
Immitzer, M., Atzberger, C., 2014. Early detection of bark beetle infestation in Norway Spruce (< I > Picea abies < /I > , L.) using worldview-2 data < BR > Frühzeitige Erkennung von Borkenkä ferbefall an Fichten mittels WorldView-2 Satellitendaten. Photogramm. - Fernerkundung - Geoinf. 2014 (5), 351–367.
Lausch, A., Fahse, L., Heurich, M., 2011. Factors affecting the spatio-temporal dispersion of Ips typographus (L.) in Bavarian Forest National Park: a long-term quantitative landscape-level analysis. For. Ecol. Manage. 261 (2), 233–245.
Lausch, A., Heurich, M., Fahse, L., 2013a. Spatio-temporal infestation patterns of Ips typographus (L.) in the Bavarian Forest National Park, Germany. Ecological Indicators 31, 73–81.
Lausch, A., Heurich, M., Gordalla, D., Dobner, H.J., Gwillym-Margianto, S., Salbach, C., 2013b. Forecasting potential bark beetle outbreaks based on spruce forest vitality using hyperspectral remote-sensing techniques at different scales. For. Ecol. Manage. 308, 76–89.
Lobinger, G., 1994. Air temperature as a limiting factor for flight activity of two species of pine bark beetles, Ips typographus L. and Pityogenes chalcographus L.(Col., Scolytidae). Anzeiger für Schädlingskunde, Pflanzenschutz, Umweltschutz 67 (1), 14–17.
Meddens, A.J., Hicke, J.A., Ferguson, C.A., 2012. Spatiotemporal patterns of observed bark beetle-caused tree mortality in British Columbia and the western United States. Ecol. Appl. 22 (7), 1876–1891.
Meddens, A.J.H., Hicke, J.A., Vierling, L.A., Hudak, A.T., 2013. Evaluating methods to detect bark beetle-caused tree mortality using single-date and multi-date landsat imagery. Remote Sens. Environ. 132, 49–58.
Meigs, G.W., Kennedy, R.E., Cohen, W.B., 2011. A Landsat time series approach to characterize bark beetle and defoliator impacts on tree mortality and surface fuels in conifer forests. Remote Sens. Environ. 115 (12), 3707–3718.
Meygret, A., 2007. SPOT Absolute Calibration: Synthesis.
Morris, J.L., Cottrell, S., Fettig, C.J., DeRose, R.J., Mattor, K.M., Carter, V.A., Clear, J., Clement, J., Hansen, W.D., Hicke, J.A., Higuera, P.E., Seddon, A.W.R., Seppä, H., Sherriff, R.L., Stednick, J.D., Seybold, S.J., 2018. Bark beetles as agents of change in social-ecological systems. Front. Ecol. Environ. 16 (S1), S34–S43.
Murtha, P., Wiart, R., 1989. PC-based digital analysis of mountain pine beetle current-attacked and non-attacked lodgepole pine. Can. J. Remote. Sens.
Murtha, P.A., 1972. Guide to Air Photo Interpretation of Forest Damage in Canada.
Näsi, R., Honkavaara, E., Blomqvist, M., Lyytikäinen-Saarenmaa, P., Hakala, T., Viljanen, N., Kantola, T., Holopainen, M., 2018. Remote sensing of bark beetle damage in urban forests at individual tree level using a novel hyperspectral camera from UAV and aircraft. Urban For. Urban Green. 30, 72–83.
Netherer, S., Schopf, A., 2010. Potential effects of climate change on insect herbivores in European forests—general aspects and the pine processionary moth as specific example. For. Ecol. Manage. 259 (4), 831–838.
Oerke, E., Steiner, U., Dehne, H., Lindenthal, M., 2006. Thermal imaging of cucumber leaves affected by downy mildew and environmental conditions. J. Exp. Bot. 57 (9), 2121–2132.
Öhrn, P., 2012. The Spruce Bark Beetle Ips typographus in a Changing Climate.
Ortiz, S., Breidenbach, J., Kändler, G., 2013. Early detection of bark beetle green attack using terraSAR-X and RapidEye data. Remote Sens. (Basel) 5 (4), 1912–1931.
Overbeck, M., Schmidt, M., 2012. Modelling infestation risk of Norway spruce by Ips typographus (L.) in the Lower Saxon Harz Mountains (Germany). For. Ecol. Manage. 266, 115–125.
Paine, T.D., Raffa, K.F., Harrington, T.C., 1997. Interactions among scolytid bark beetles, their associated Fungi, and live host conifers. Annu. Rev. Entomol. 42 (1), 179–206.
Pinder, J.E., McLeod, K.W., 1999. Indications of relative drought stress in longleaf pine from thematic mapper data. Photogramm. Eng. Remote Sensing 65 (4), 495–501.
Pu, R., Gong, P., 2011. Hyperspectral remote sensing of vegetation bioparameters. Advances in environmental remote sensing: Sensors, algorithms, and applications 7. pp. 101–142.
Raffa, K.F., Aukema, B.H., Bentz, B.J., Carroll, A.L., Hicke, J.A., Turner, M.G., Romme, W.H., 2008. Cross-scale drivers of natural disturbances prone to anthropogenic amplification: the dynamics of bark beetle eruptions. BioScience 58 (6), 501–517.
RapidEye, A., 2011. RapidEye Standard Image Product Specifications. RapidEye AG: Brandenburg an der Havel, Germany, pp. 1–54.
Rohde, M., Waldmann, R., Lunderstädt, J., 1996. Induced defence reaction in the phloem of spruce (Picea abies) and larch (Larix decidua) after attack by Ips typographus and Ips cembrae. For. Ecol. Manage. 86 (1), 51–59.
Seidl, R., Schelhaas, M.-J., Lexer, M.J., 2011. Unraveling the drivers of intensifying forest disturbance regimes in Europe. Glob. Chang. Biol. 17 (9), 2842–2852.
Skakun, R.S., Wulder, M.A., Franklin, S.E., 2003. Sensitivity of the thematic mapper enhanced wetness difference index to detect mountain pine beetle red-attack damage. Remote Sens. Environ. 86 (4), 433–443.
Slaton, M.R., Raymond Hunt Jr., E., Smith, W.K., 2001. Estimating near-infrared leaf reflectance from leaf structural characteristics. Am. J. Bot. 88 (2), 278–284.
Thom, D., Seidl, R., 2016. Natural disturbance impacts on ecosystem services and biodiversity in temperate and boreal forests. Biol. Rev. Camb. Philos. Soc. 91 (3), 760–781.
Tucker, C.J., 1979. Red and photographic infrared linear combinations for monitoring vegetation. Remote Sens. Environ. 8 (2), 127–150.
Tyc, G., Tulip, J., Schulten, D., Krischke, M., Oxfort, M., 2005. The RapidEye mission design. Acta Astronaut. 56, 213–219.
Vincini, M., Frazzi, E., D'Alessio, P., 2008. A broad-band leaf chlorophyll vegetation index at the canopy scale. Precis. Agric. 9 (5), 303–319.
Wermelinger, B., 2004. Ecology and management of the spruce bark beetle Ips typographus—a review of recent research. For. Ecol. Manage. 202 (1–3), 67–82.
Westfall, J., Ebata, T., 2009. 2008. Summary of Forest Health Conditions in British Columbia. British Columbia ministry of Forests and Range. Pest Management Report.
White, J., Coops, N., Hilker, T., Wulder, M., Carroll, A., 2007. Detecting mountain pine beetle red attack damage with EO-1 hyperion moisture indices. Int. J. Remote Sens. 28 (10), 2111–2121.
White, J.C., Wulder, M.A., Grills, D., 2006. Detecting and mapping mountain pine beetle red-attack damage with SPOT-5 10-m multispectral imagery. J. Ecosyst. Manage. 7 (2).
Wulder, M.A., White, J.C., Bentz, B., Alvarez, M.F., Coops, N.C., 2006. Estimating the probability of mountain pine beetle red-attack damage. Remote Sens. Environ. 101 (2), 150–166.
Wulder, M.A., White, J.C., Carroll, A.L., Coops, N.C., 2009. Challenges for the operational detection of mountain pine beetle green attack with remote sensing. For. Chron. 85 (1), 32–38.
Yamaoka, Y., Swanson, R., Hiratsuka, Y., 1990. Inoculation of lodgepole pine with four blue-stain fungi associated with mountain pine beetle, monitored by a heat pulse velocity (HPV) instrument. Can. J. For. Res. 20 (1), 31–36.
Zhang, Y., Chen, J.M., Miller, J.R., Noland, T.L., 2008. Leaf chlorophyll content retrieval from airborne hyperspectral remote sensing imagery. Remote Sens. Environ. 112 (7), 3234–3247.
Zweifel, R., Rigling, A., Dobbertin, M., 2009. Species-specific stomatal response of trees to drought–a link to vegetation dynamics? J. Veg. Sci. 20 (3), 442–454.